



Solubility and sorption of redox-sensitive radionuclides (Np, Pu) in J-13 water from the Yucca Mountain site: comparison between experiment and theory

Wolfgang Runde*, Steve D. Conradson, D. Wes Efurud,
NingPing Lu, Craig E. VanPelt, C. Drew Tait

Chemical, Science and Technology Division, CST-7, Mail Stop J514, Los Alamos National Laboratory, Los Alamos, NM 87545, USA

Received 3 November 2000; accepted 25 July 2001

Editorial handling by M. Gascoyne

Abstract

This study presents the characterization of Pu-bearing precipitates and the results from uptake studies of Np and Pu on inorganic colloidal particulates in J-13 water from the Yucca Mountain site. Plutonium solubilities determined experimentally at pH values of 6, 7, and 8.5 are about two orders of magnitude higher than those calculated using the existing thermodynamic database indicating the influence of colloidal Pu(IV) species. Solid phase characterization using X-ray diffraction revealed primarily Pu(IV) in all precipitates formed at pH 6, 7, and 8.5. The solubility controlling Pu-bearing solids precipitated at ambient temperature consisted of amorphous Pu(OH)₄(s) with several Pu–O distances between 2.3 and 2.7 Å that are characteristic for Pu(IV) colloids. High temperature (90 °C) increased solid phase crystallinity and produced Pu(IV) solids that contained Pu oxidation state impurities. X-ray absorption spectroscopic studies revealed diminished Pu–O and Pu–Pu distances that were slightly different from those in crystalline PuO₂(s). A Pu–O bond of 1.86 Å was identified that is consistent with the plutonyl(V) distance of 1.81 Å in PuO₂⁺(aq). Hematite, montmorillonite, and silica colloids were used for uptake experiments with ²³⁹Pu(V) and ²³⁷Np(V). The capacity of hematite to sorb Pu significantly exceeded that of montmorillonite and silica. A low desorption rate was indicative of highly stable Pu-hematite colloids, which may facilitate Pu transport to the accessible environment. Neptunium uptake on all mineral phases was far less than Pu(V) uptake suggesting that a potential Pu(V)–Pu(IV) reductive sorption process was involved. The temperature effect on Pu solubility and pseudocolloid formation is also discussed. © 2002 Published by Elsevier Science Ltd.

1. Introduction

The Yucca Mountain site in Nevada is currently under investigation as a potential location for the disposition of high-level nuclear waste (DOE, 1988). Risk and safety assessment must consider the potential worst-case scenario of water intrusion into the repository and the subsequent dissolution and transport of radionuclides into the environment. Groundwater flow through the waste is expected to be slow (Craig, 1999), and saturation of the infiltrating water with radionuclides

dissolved from the waste package could occur. Processes such as dissolution kinetics, solubility, solution speciation, and molecular-scale reactions at solid-water interfaces define the radionuclide source term for transport calculations.

Neptunium and plutonium are the primary actinides of fundamental concern for long-term storage of nuclear waste due to their long half-lives ($t_{1/2} = 2.14 \times 10^6$ a for ²³⁷Np and 2.41×10^4 a for ²³⁹Pu), radiotoxicity, and reportedly different transport characteristics under varying conditions (Dozol et al., 1993). Both radioelements are redox-sensitive with two or more stable oxidation states under conditions to be expected at Yucca Mountain. Neptunium tends to be stable as NpO₂⁺ in the

* Corresponding author. Fax: +1-505-665-4955.
E-mail address: runde@lanl.gov (W. Runde).

pentavalent oxidation state under a wide range of environmental conditions. Due to its high solubility and low sorption affinity, Np(V) is considered to be the most environmentally mobile actinide species (Choppin, 1983). The chemistry of Pu is more complex, and it can exist in the III, IV, V, and VI oxidation states with lower solubility and mobility for the lower oxidation states III and IV.

Radionuclide transport from a storage or disposal site is controlled by the various site-specific chemical (i.e. nature and concentration of ligands, pH, Eh, and amounts of colloidal matter) and physical (i.e. temperature and pressure) conditions within the isolated waste-package and the surrounding environment. The primary variable that determines the migration of an actinide element is its oxidation state. Typically, spent nuclear fuel contains the actinides in their low oxidation states within a UO₂ matrix. Reducing conditions in the repository should retain the actinides in their low oxidation states with generally low solubilities. Oxidizing waters from the surrounding environment may infiltrate the waste disposal area, and redox-sensitive actinides could be oxidized to their more soluble higher oxidation states. The dissolved actinides may undergo immobilization by (co)precipitation of secondary phases or by sorption onto corroded waste packages or mineral phases but may also be transported into the environment as molecular solution species or sorbed onto colloidal particulates.

A broad range of geochemical processes and chemical conditions that control solubility, oxidation-state stability, and solution speciation must be considered in release scenarios of actinides. In laboratory studies, only individual reactions under site-specific conditions are investigated and geochemical modeling efforts examine interactions under expected conditions. The aim of this work was to investigate the precipitation of secondary Pu-bearing solid phases and its consequences for overall Pu solubility. Pu solubility experiments were performed in J-13 water from oversaturation at 25, 60, and 90 °C and characterized the precipitated solid phase by X-ray diffraction and X-ray absorption spectroscopy. The sorption of Np and Pu to colloids potentially produced by waste package degradation and to naturally occurring mineral colloids in groundwater was explored as a viable transport mechanism. Laboratory batch experiments were conducted to evaluate the adsorption kinetics onto hematite, montmorillonite, and silica colloids and the effect of temperature, ionic strength, and colloid concentration on the overall phase participation.

2. Methodology

2.1. Solubility studies and solid phase characterization

For both solubility and sorption studies, water from well J-13 at Fortymile Wash, east of the Yucca

Mountain site, Nevada, was used. This well water is low in ionic strength, and the main ligands present for actinide complexation are carbonate and hydroxide (Table 1). J-13 water is considered as reference water for the saturated zone near the proposed emplacement area (Nitsche et al., 1992).

The experimental approach to determine Np and Pu solubility in J-13 water was described in detail previously (Efurd et al., 1998). Experiments were performed from oversaturation at 3 temperatures (25, 60, and 90 °C) at pH values of 6, 7, and 8.5 while purging the system with the appropriate CO₂/Ar mixture to adjust the total carbonate concentration at 2.8 mmol/l. The Pu concentrations in solution were determined by α -scintillation counting after filtration of the solution aliquots with 4.1 nm pore-size filters. The solubility-controlling solid precipitates were separated by centrifugation for analysis after about 400 days of reaction time. In addition to X-ray diffraction and diffuse reflectance spectroscopy (Efurd et al., 1998), X-ray absorption spectroscopy (XAS) was used to obtain structural information on the Pu solids. The solid Pu sample was mounted in the interior of a sample holder that was doubly contained with Kapton film. XAS data were recorded at 295 K at the Stanford Synchrotron Radiation Laboratory (SSRL) on the unfocused wiggler beamline 4-2 with an electron beam energy of 3.0 GeV and beam currents between 60 and 100 mA. A Si(220) double-crystal monochromator was used. The X-ray absorption near-edge region (XANES) was taken as extending above the Pu edge to 18120 eV. The spectra were energy calibrated against the spectrum for Zr foil by defining the first inflection point as the Zr K-edge at 17999.35 eV. The data were analyzed using in-house data analysis programs. The Pu L_{III} edge data were normalized by setting the value of a second-order polynomial fit through the pre-edge region to zero at E_0 and to unity through the extended X-ray absorption fine structure (EXAFS) region at 18120 eV. A cubic spline function was used to fit the background over the EXAFS region, which extended to $k = 11.7 \text{ \AA}^{-1}$. Fourier transforms of the raw k^3 -weighted EXAFS data were calculated over the range $k = 3.0\text{--}11.7 \text{ \AA}^{-1}$. Theoretical phases and amplitudes were derived from the program FEFF7 (Ankudinov and Rehr, 1997) to fit the contributions from the O neighbor atoms. The parameters refined in the fit were: the photoelectron energy threshold (ΔE_0); the distance (R_i) to the Pu center and number (n_i) of i atoms; and the Debye-Waller factor (σ_i) for atom i . The quality of the fit was determined by the residual between the fit and k -space data.

2.2. Sorption studies

Colloidal solutions of hematite (particle size <1.0 μm , Nissan Chemical Industries, Ltd.) and montmor-

Table 1
Composition of water from well J-13 at the Yucca Mountain site (Harrar et al., 1990)

Species	Concentration (mM)	Species	Concentration (mM)
Na ⁺	1.99	F ⁻	0.11
K ⁺	0.129	Cl ⁻	0.20
Li ⁺	0.009	NO ₃ ⁻	0.14
Ca ²⁺	0.324	SO ₄ ²⁻	0.19
Mg ²⁺	0.083	SiO ₂	1.02
Mn ²⁺	> 0.0001	Alkalinity ^a	2.1
Fe ^{2+/3+}	> 0.001		
pH	7.4	Eh ^b	430 mV

^a Alkalinity was determined as HCO₃⁻ by acid titration.

^b The redox potential of J-13 water at a pH of 7 and the Ar/CO₂ gas mixture used in the solubility experiments was measured with a combined redox and Ag/AgCl reference electrode (Orion, Model 96–78–00) (Efurd et al., 1998).

illonite (particle size < 1.0 μm, University of Missouri, Columbia, Source Clay Mineral Repository, Clay Mineral Society) were prepared by dispersing the corresponding powder in nanopure deionized water using an ultrasonic bath for 3 min. Remaining large particles were allowed to settle for 5 h in a 1-L cylinder at room temperature. The supernatants (pH = 6.9) were carefully collected as the stock colloidal solutions. The colloidal mass per solution volume was determined by weight difference of a colloidal suspension aliquot before and after evaporation under both ambient temperature and 105 °C. Colloidal suspensions of 200 mg l⁻¹, as used in the experiments, were prepared by diluting the colloid stock solution into one liter of J-13 water. Amorphous synthetic colloidal silica (Nissan Chemical Industries, Ltd.) was dispersed in nanopure deionized water (40% SiO₂ and 60% water). To clean the colloidal silica from surfactants (mainly Na₂O), 50 ml of original colloidal solution was diluted to 200 ml with nanopure water and purified in a sealed dialysis tube with a 12,000–14,000 molecular weight cut-off membrane for 50 days. The removal of Na, K, and Ca was confirmed by conductivity measurements performed before and after the dialysis process. Aggregation of silica colloidal particles in the experimental colloidal solution occurred after 6 months. The particle size and surface charge (zeta potential) of hematite, montmorillonite, and silica colloids were measured using a light-scattering system (LS-300, Coulter) and a mobility measuring system (Delsa 440 SX, Coulter), respectively. Total surface area was measured using the sorption procedure of ethylene glycol monoethylether (EGME) described in Carter et al. (1986). The results of the characterization of the colloidal solutions are summarized in Table 2.

Batch sorption experiments were performed in duplicate under atmospheric conditions using ²³⁹Pu(V) and

Table 2
Characterization of colloidal hematite, Ca-montmorillonite, and silica J-13 solutions

	Hematite	Montmorillonite	Silica
pH	8.19	8.22	8.20
Mass of colloids (mg L ⁻¹)	200	200	200
Average particle size (nm)	70	100	100
Average zeta potential (mV)	-14.1 ± 14.1	-11.7 ± 9.8	-31.0 ± 7.3
Total surface area (m ² kg ⁻¹)	5.4 × 10 ⁴	8.3 × 10 ⁵	1.1 × 10 ⁶

²³⁷Np(V) and colloidal solutions of hematite, montmorillonite, and silica. Two radionuclide stock solutions, 7.66 × 10⁻⁴ M in ²³⁹Pu(V) and 0.025 M in ²³⁷Np(V), were prepared by dissolving the corresponding solid hydroxide in 0.1 M HClO₄. Spectroscopic analysis of the stock solutions resulted in 99.7% Pu(V) (absorbance at 569 nm) and 0.3% Pu(VI) (absorbance at 830 nm) for the Pu solution, and pure Np(V) (absorbance at 981 nm) for the Np solution. Aliquots of these stock solutions were diluted in J-13 water to obtain 2.74 × 10⁻⁷ M Pu(V) and 1.90 × 10⁻⁷ M Np(V) working solutions. One-ml aliquots of these working solutions were added to 20 ml of J-13 water that contained 200 mg/l hematite, montmorillonite, or silica colloids. The samples were placed on an orbital shaker at 150 rpm. In parallel, control samples with the same Pu or Np concentrations but no colloidal particles were prepared. After 1, 4, 24, 48, 96, and 240 h of contact time, the samples were centrifuged for 4 h at 38,300 g. The supernatant was separated, the pH was measured, and the Pu and Np concentrations were determined using liquid scintillation counting. Results from the control samples were used to correct for sorption onto container surfaces. The sorption distribution coefficient (*K_d*) was calculated using the following equation:

$$K_d(\text{ml/g}) = [(A_0 V_0 - A_t V_t)/m]/A_t \quad (1)$$

where *A*₀ is the initial concentration of ²³⁹Pu or ²³⁷Np per ml of solution; *V*₀ is the initial solution volume (ml) in contact with the colloidal particles; *A*_{*t*} is the concentration of ²³⁹Pu or ²³⁷Np per ml solution at time *t* after the measured sorption is corrected for sorption on the container walls; *V*_{*t*} is the solution volume (ml) in contact with the colloidal particles after sorption; and *m* is the mass (g) of colloids used in each sorption experiment.

To investigate the effect of temperature on Np and Pu sorption, a set of experiments was performed as described above at 20, 40, and 80 °C in a temperature-controlled sample compartment. Separation and analysis of

the supernatant was conducted after 240 h contact time. Plutonium- and Np-loaded colloids separated from the 20 °C experiment were combined with 10 ml of fresh J-13 water to study the reversibility of the sorption process. Desorption of Np and Pu proceeded for 212 days and 293 days, respectively. After separation of the colloidal fraction by centrifugation, the supernatant was analyzed for Np and Pu activity using liquid scintillation counting.

2.3. Geochemical modeling

Geochemical modeling and thermodynamic calculations were performed with the software *Geochemist's Workbench*, version 3.0 (Bethke, 1998), using the b-dot extended Debye-Huckel model for activity coefficient calculations and the thermodynamic database DATA0.COM.V8.R6 (LLNL, December 1996). This database relies on Np data from Lemire and Garisto (1989) and Pu data from Lemire and Tremaine (1980). Because the compilation and assessment of available thermodynamic data for the Np system was reported earlier (Kaszuba and Runde, 1999), the authors concentrated on the Pu system. Current literature thermodynamic data was compiled for solid and solution Pu compounds that are most likely to dominate Pu speciation in natural waters. The Gibbs free energies of formation (ΔG_{298}°) of these compounds were calculated after correcting for ionic strength at standard conditions. These data were incorporated into the existing database. For ionic strength corrections, the theory of specific ion-interaction (S.I.T.) (Grenthe et al., 1992) was used because little data were available for the more sophisticated Pitzer model. Lemire's data was adapted without reevaluation for Pu species that are not likely to be important in dilute, repository-equivalent waters, i.e. nitrates or sulfates. Plutonium species with no experimental evidence of formation or that lack characterization were deleted from the existing database and not used in the calculations. The thermodynamic data used in this work are summarized in Table 3, and a short discussion is provided below.

2.4. Analysis of thermodynamic data of plutonium

The Pu species most relevant for low ionic strength Conditions of natural waters are, in solution, the aqueous ions, hydroxides, carbonates, and F solution species, and in the solid state, oxides, hydroxides, and carbonates. Due to the low ligand concentrations, SO_4^{2-} , NO_3^- , PO_4^{3-} and Cl^- are not important in most natural waters. Thermodynamic stability constants and the Gibbs free energies of formation, $\Delta_f G_{298}^{\circ}$, reported in peer-reviewed journals were reviewed and compiled in Table 3 for use in the calculations. A detailed review of the aqueous chemistry of Pu is outside the range of this

paper, and the reader is referred to the numerous reviews in the literature (Cleveland, 1979; Choppin, 1983; Katz et al., 1986).

2.4.1. Plutonium aqueous ions

The oxidation states of Pu relevant under most environmental conditions are III, IV, V, and VI. The formal potentials for the $\text{Pu}^{4+}/\text{Pu}^{3+}$ and $\text{PuO}_2^{2+}/\text{PuO}_2^+$ couples were measured at 25 °C and corrected for ionic strength obtaining $E^{\circ}=1.044\pm 0.010$ V and $E^{\circ}=0.938\pm 0.010$ V, respectively (Capdevila et al., 1992; Capdevila and Vitorge, 1995). The recommended $\Delta_f G_{298}^{\circ}(\text{Pu}^{3+})=-578.6\pm 3.3$ kJ mol⁻¹ (Fuger and Oetting, 1976) was used for the subsequent calculations of the Gibbs free energies of Pu^{4+} , PuO_2^+ , and PuO_2^{2+} . $\Delta_f G_{298}^{\circ}(\text{Pu}^{4+})$ was determined from $E^{\circ}(\text{Pu}^{4+}/\text{Pu}^{3+})$ and $\Delta_f G_{298}^{\circ}(\text{Pu}^{3+})$ to be -477.9 ± 3.4 kJ mol⁻¹. $\Delta_f G_{298}^{\circ}(\text{PuO}_2^+)$ was calculated from $\Delta_f G_{298}^{\circ}(\text{Pu}^{3+})$ and the standard potential $E^{\circ}=1.014\pm 0.025$ V for the reaction $\text{PuO}_2^+ + 4\text{H}^+ + 2\text{e}^- \rightleftharpoons \text{Pu}^{3+} + 2\text{H}_2\text{O}(\text{aq})$ (Capdevila et al., 1992; Capdevila and Vitorge, 1995). $\Delta_f G_{298}^{\circ}(\text{PuO}_2^{2+})=-766.8\pm 6.6$ kJ mol⁻¹ was calculated from the standard potential for the $\text{PuO}_2^{2+}/\text{PuO}_2^+$ couple and $\Delta_f G_{298}^{\circ}(\text{PuO}_2^+)$. The data compiled here differ slightly from those previously used to model Pu geochemistry [$E^{\circ}(\text{PuO}_2^{2+}/\text{PuO}_2^+)=+1.016\pm 0.05$ V and $E^{\circ}(\text{Pu}^{4+}/\text{Pu}^{3+})=+1.006\pm 0.03$ V; $\Delta_f G_{298}^{\circ}(\text{PuO}_2^{2+})=-756.9\pm 7.1$ kJ mol⁻¹, $\Delta_f G_{298}^{\circ}(\text{PuO}_2^+)=-849.8\pm 7.5$ kJ mol⁻¹, $\Delta_f G_{298}^{\circ}(\text{Pu}^{4+})=-481.6\pm 3.3$ kJ mol⁻¹, $\Delta_f G_{298}^{\circ}(\text{Pu}^{3+})=-578.6\pm 3.3$ kJ mol⁻¹ (Fuger, 1972; Lemire and Tremaine, 1980)]. The main differences between the two data sets originate from the method of correction for ionic strength.

2.4.2. Plutonium hydroxides

Pu(III). The difficulty of maintaining Pu(III) complicates the accurate determination of thermodynamic data. The authors accepted the data from potentiometric titration experiments (Kraus and Dam, 1949) because of the methods implemented to control Pu(III) oxidation. Ionic strength was corrected for using S.I.T. parameters from the analogous lanthanide system to calculate $\log\beta_{11}^{\circ}=-7.0\pm 0.4$ for $\text{Pu}(\text{OH})_2^{2+}$.

Pu(IV). The investigation and accurate determination of Pu(IV) hydrolysis species is extremely complicated by the formation of colloidal Pu(IV) species and the dependence of Pu redox reactions on ionic strength, pH, and time. The $\text{Pu}(\text{OH})_3^{3+}$ stability constant averaged from potentiometric (Rabideau and Lemons, 1951; Rabideau, 1957) and spectroscopic (Nitsche and Silva, 1996) studies and corrected for ionic strength (using the S.I.T. ion-interaction parameters of $\text{U}(\text{OH})_3^{3+}$; Grenthe et al., 1992) resulted in $\log\beta_{11}^{\circ}=-0.5\pm 0.4$. The thermodynamic data of $\text{U}(\text{OH})_4(\text{aq})$, $\Delta_f G_{298}^{\circ}=-1452.5\pm 8$ kJ mol⁻¹ (Grenthe et al., 1992), and $\text{Np}(\text{OH})_4(\text{aq})$, $\Delta_f G_{298}^{\circ}=-1382.7\pm 11.1$ kJ mol⁻¹ (Kaszuba and Runde,

Table 3

Standard redox potentials, thermodynamic stability constants, and $\Delta_r G_{298}^\circ$ values (of species in bold) for environmentally relevant Pu compounds^a

Species / Reaction	E° (V)	log K° or log β°	$\Delta_r G_{298}^\circ$ (kJ mol ⁻¹)
Pu⁴⁺ / Pu³⁺	1.044±0.010	–	–
PuO₂²⁺ / PuO₂⁺	0.938±0.010	–	–
Pu³⁺	–	–	–578.6±3.3
Pu⁴⁺	–	–	–477.9±3.4
PuO₂⁺	–	–	–857.3±6.7
PuO₂²⁺	–	–	–766.8±6.6
Pu³⁺ + H₂O = PuOH²⁺ + H⁺		–7.0±0.4	–775.8±4.0
Pu³⁺ + CO₃²⁻ = Pu(CO₃)⁺		8.1±0.3	–1152.8±3.7
Pu³⁺ + 2 CO₃²⁻ = Pu(CO₃)₂⁻		12.9±0.4	–1708.2±4.0
Pu³⁺ + 3 CO₃²⁻ = Pu(CO₃)₃²⁻		15.4±0.6	–2250.4±4.8
Pu⁴⁺ + H₂O = PuOH³⁺ + H⁺		0.6±0.2	–718.5±3.6
Pu⁴⁺ + 2 H₂O = Pu(OH)₂²⁺ + 2 H⁺		0.6±0.3	–955.7±3.8
Pu⁴⁺ + 3 H₂O = Pu(OH)₃⁺ + 3 H⁺		–2.3±0.4	–1176.3±4.1
Pu⁴⁺ + 4 H₂O = Pu(OH)₄(aq) + 4 H⁺		–8.6±0.5	–1377.5±4.5
Pu⁴⁺ + 4 CO₃²⁻ = Pu(CO₃)₄⁻		34.1±1.3	–2784.5±8.1
Pu⁴⁺ + 5 CO₃²⁻ = Pu(CO₃)₅²⁻		32.7±1.3	–3304.4±8.1
PuO₂⁺ + H₂O = PuO₂OH(aq) + H⁺		–9.7±0.1	–1039.1±6.7
PuO₂⁺ + CO₃²⁻ = PuO₂CO₃		5.1±0.1	–1414.4±6.7
PuO₂⁺ + 2 CO₃²⁻ = PuO₂(CO₃)₂⁻		6.5±0.2	–1950.4±6.8
Estimated from NpO ₂ (CO ₃) ₂ ⁻			
PuO₂⁺ + 3 CO₃²⁻ = PuO₂(CO₃)₃²⁻		5.5±0.2	–2472.6±6.8
Estimated from NpO ₂ (CO ₃) ₃ ²⁻			
PuO₂²⁺ + H₂O = PuO₂OH⁺ + H⁺		8.5±0.2	–972.6±6.7
PuO₂²⁺ + 2 H₂O = PuO₂(OH)₂(aq) + H⁺		14.8±0.3	–1165.9±6.8
PuO₂²⁺ + CO₃²⁻ = PuO₂CO₃(aq)		9.4±0.3	–1348.4±6.8
PuO₂²⁺ + 2 CO₃²⁻ = PuO₂(CO₃)₂⁻		15.0±0.5	–1908.4±7.2
PuO₂²⁺ + 3 CO₃²⁻ = PuO₂(CO₃)₃²⁻		17.5±0.4	–2450.6±7.0
Pu⁴⁺ + F⁻ = PuF³⁺		8.8±0.5	–809.9±4.5
Pu⁴⁺ + 2 F⁻ = PuF₂²⁺		15.8±0.5	–1131.6±4.6
PuO₂⁺ + F⁻ = PuO₂F⁺		4.7±0.2	–1075.4±6.7
PuO₂²⁺ + 2 F⁻ = PuO₂F₂(aq)		7.2±0.5	–1371.4±7.2
Pu(OH)₃(s) = Pu³⁺ + 3 OH⁻		–26.2±0.8	–1200.0±5.7
Pu(OH)CO₃(s) = Pu³⁺ + OH⁻ + CO₃²⁻		–21.2±1.4	–1227.6±8.7
PuO₂·2H₂O = Pu⁴⁺ + 4 OH⁻			
or Pu(OH) ₄ (am) = Pu ⁴⁺ + 4 OH ⁻		–58.5±1.0	–1441.0±6.6
PuO₂(c) + 2 H₂O = Pu⁴⁺ + 4 OH⁻		v63.8±1.0	–1471.3±6.6
PuO₂(OH)(am) = PuO₂⁺ + OH⁻		–8.9±0.3	–1065.4±6.9
PuO₂(OH)₂(s) = PuO₂²⁺ + 2 OH⁻		–22.7±1.0	–1211.0±8.7
PuO₂CO₃(s) = PuO₂²⁺ + CO₃²⁻		–14.3±0.5	–1376.4±7.2
H ₂ O(aq)	–	–	–237.18±0.08
OH ⁻	–	–	–157.30±0.09
CO ₃ ²⁻	–	–	–527.98±0.12
HCO ₃ ⁻	–	–	–586.94±0.12
F ⁻	–	–	–281.75±0.67

^a $\Delta_r G_{298}^\circ$ values of auxiliary species used in the calculations are also provided. Superscript zero (°) indicates the thermodynamic standard state, defined as the stable state at 1 bar pressure and the temperature under consideration (25 °C). Uncertainties for $\Delta_r G_{298}^\circ$ of Pu compounds arise from error propagation in converting from log K° or log β° to $\Delta_r G_{298}^\circ$.

1999), were used to estimate $\Delta_r G_{298}^\circ(\text{Pu}(\text{OH})_4(\text{aq})) = -1375 \pm 23 \text{ kJ mol}^{-1}$ and $\log \beta_{14}^\circ = -9 \pm 1$. These values are in good agreement with the extraction data of ^{238}Pu (Metivier and Guillaumont, 1972; 1976). For internal consistency, the authors adopted their set of apparent stability constants and corrected for ionic strength using S.I.T. parameters of the analogue U(IV) hydrolysis system and $\epsilon(\text{Pu}^{4+}/\text{ClO}_4^-) = 0.84 \pm 0.2$ (Capdevila and Vitorge, 1998) to obtain $\log \beta_{11}^\circ = 0.6 \pm 0.2$, $\log \beta_{12}^\circ = 0.6 \pm 0.3$, $\log \beta_{13}^\circ = -2.3 \pm 0.4$, and $\log \beta_{14}^\circ = -8.6 \pm 0.5$.

Pu(V). The formation constant of $\text{PuO}_2\text{OH}(\text{aq})$ was determined by laser-induced photoacoustic spectroscopy as $\log \beta_{11}^\circ = -9.73 \pm 0.10$ (Bennett et al., 1992) which agreed well with the former $\log \beta_{11}^\circ = -9.7$ (Kraus and Nelson, 1948).

Pu(VI). The formation constants for PuO_2OH^+ and $\text{PuO}_2(\text{OH})_2(\text{aq})$ were determined spectroscopically as $\log \beta_{11}^\circ = 8.52$ and $\log \beta_{12}^\circ = 14.64$ (Pashalidis et al., 1995). The U(VI)–OH S.I.T. parameters (instead of those for the U(VI)–F reactions) were used to calculate $\log \beta_{11}^\circ = 8.5 \pm 0.2$ and $\log \beta_{12}^\circ = 14.8 \pm 0.3$. While the Pu solubility increases at high pH, indicating the formation of anionic Pu(VI) hydroxo complexes, no reliable thermodynamic data for those species or polynuclear species are available in the current literature.

2.4.3. Plutonium carbonates

Pu(III). Formation constants have been estimated for the Pu(III) carbonate complexes PuCO_3^+ and $\text{Pu}(\text{CO}_3)_2^-$ by analogy with the trivalent lanthanides (Cantrell, 1988). As a guideline, the averaged stability constants of the Am(III) (Silva et al., 1995) and Cm(III) (Fanghänel et al., 1999) carbonate complexes can be used: $\log \beta_{11}^\circ = 8.1 \pm 0.3$, $\log \beta_{12}^\circ = 12.9 \pm 0.4$, and $\log \beta_{13}^\circ = 15.4 \pm 0.6$.

Pu(IV). Although crystallographic data exist on the pentacarbonato complex, $\text{M}(\text{CO}_3)_5^{6-}$ ($\text{M} = \text{Th}, \text{U}, \text{Np}, \text{Pu}$), quantitative studies on the thermodynamics are lacking. We accepted the recently published value for $\log \beta_{15}(\text{Pu}(\text{CO}_3)_5^{6-}) = 35.8 \pm 1.3$ at ionic strength $I = 3 \text{ M}$ (Capdevila et al., 1996) and obtained $\log \beta_{15}^\circ = 32.7 \pm 1.3$ by using $\epsilon(\text{U}(\text{CO}_3)_5^{6-}/\text{ClO}_4^-) = -0.30 \pm 0.15$ (Silva et al., 1995) and $\epsilon(\text{Pu}^{4+}/\text{ClO}_4^-) = 0.84 \pm 0.2$ (Capdevila and Vitorge, 1998). The stepwise constant $\log K_{15}^\circ = -1.36 \pm 0.09$ (Capdevila et al., 1996) was used to obtain $\log \beta_{14}(\text{Pu}(\text{CO}_3)_4^{4-}) = 34.1 \pm 1.3$. The stepwise constant is in good agreement with that for the analogue U(IV) compound, $\log K_{15}^\circ = -1.12 \pm 0.25$ (Grenthe et al., 1992). Reliable formation constants for other Pu(IV) carbonate complexes are currently not available, and further experimental work is required. Specifically, the formation and the existence of mixed Pu(IV) hydroxocarbonate species need to be verified.

Pu(V). The constant $\log \beta_{11}^\circ(\text{PuO}_2\text{CO}_3^-) = 5.12 \pm 0.07$ was determined spectroscopically (Bennett et al., 1992) and agrees well with that of $\text{NpO}_2\text{CO}_3^-$, $\log \beta_{11}^\circ =$

4.8 ± 0.2 (Kaszuba and Runde, 1999). The formation constant of $\text{PuO}_2(\text{CO}_3)_3^{5-}$ can be estimated from the stability constant of $\text{PuO}_2(\text{CO}_3)_3^{4-}$ and the potential of the Pu(VI)/Pu(V) couple as $\log \beta_{13}^\circ = 4.9 \pm 0.7$. This value is slightly lower than that of the analogous Np(V) species. $\log \beta_{12}^\circ(\text{NpO}_2(\text{CO}_3)_3^{3-}) = 6.5 \pm 0.2$ and $\log \beta_{13}^\circ(\text{NpO}_2(\text{CO}_3)_3^{5-}) = 5.5 \pm 0.2$ (Kaszuba and Runde, 1999) were used as first estimates for $\text{PuO}_2(\text{CO}_3)_3^{3-}$ and $\text{PuO}_2(\text{CO}_3)_3^{5-}$.

Pu(VI). Analogous to the U(VI) system, experimental data suggest the existence of at least 3 Pu(VI) carbonate species, $\text{PuO}_2(\text{CO}_3)_n^{2-2n}$ where $n = 1-3$. The $\text{PuO}_2(\text{CO}_3)(\text{aq})$ formation constants from two Pu(VI) solubility studies in 3.5 M NaClO_4 (Robouch and Vitorge, 1987) and in 0.1 M NaClO_4 (Pashalidis et al., 1997) were averaged to obtain $\log \beta_{11}^\circ = 9.4 \pm 0.3$. Formation constants of $\text{PuO}_2(\text{CO}_3)_2^{2-}$ and $\text{PuO}_2(\text{CO}_3)_3^{4-}$ were determined in solubility (Robouch and Vitorge, 1987; Pashalidis et al., 1997) and calorimetry studies (Ullman and Schreiner, 1988). The S.I.T.-corrected constants were averaged to obtain $\log \beta_{12}^\circ = 15.0 \pm 0.5$ and $\log \beta_{13}^\circ = 17.5 \pm 0.4$. Note that the data for $\text{PuO}_2(\text{CO}_3)(\text{aq})$ agree well with the analogous U(VI) data, $\log \beta_{11}^\circ = 9.68 \pm 0.04$ (Grenthe et al., 1992), whereas enormous discrepancies of up to 4 orders of magnitude occur with the formation constants of the anionic U(VI) complexes, $\log \beta_{12}^\circ = 16.94 \pm 0.12$ and $\log \beta_{13}^\circ = 21.60 \pm 0.05$ (Grenthe et al., 1992).

2.4.4. Plutonium fluorides

Pu(III) and Pu(V). No reliable data on F^- complexes of Pu^{3+} and PuO_2^+ are available.

Pu(IV). Reported formation constants for PuF_3^+ and PuF_2^{2+} (Krylov and Komarov, 1969; Bagawde et al., 1976; Nash and Cleveland, 1984) were averaged to obtain $\log \beta_{11}^\circ = 8.8 \pm 0.5$ and $\log \beta_{12}^\circ = 15.8 \pm 0.6$ using $\log K = 3.18$ for the reaction $\text{H}^+ + \text{F}^- = \text{HF}$ (Grenthe et al., 1992). The value obtained agrees well with the recommended value of $\log \beta_{11}^\circ = 8.42 \pm 0.11$ (Fuger, 1992).

Pu(VI). The S.I.T.-corrected formation constants for PuO_2F^+ determined recently ($\log \beta_{11}^\circ = 4.8 \pm 0.2$, Chopin and Rao, 1984 and 4.5 ± 0.2 , Sawant et al., 1985) were averaged to obtain $\log \beta_{11}^\circ = 4.7 \pm 0.2$. The S.I.T.-corrected formation constant for $\text{PuO}_2\text{F}_2(\text{aq})$, $\log \beta_{12}^\circ = 7.2 \pm 0.5$ (Sawant et al., 1985), differs slightly from the recommended value of $\log \beta_{12}^\circ = 8.24 \pm 0.10$ (Fuger, 1992).

2.4.5. Other plutonium solution species

The most important inorganic ligands of secondary priority are Cl^- , PO_4^{3-} , SO_4^{2-} and NO_3^- . The corresponding solids are so soluble (with the exception of PO_4^{3-} compounds) that their formation in common natural environments can be neglected.

Phosphates. Phosphate forms strong complexes with Pu ions in all oxidation states. We adopted the

recommended value of $\log\beta_1^\circ = 2.5 \pm 0.1$ for $\text{Pu}(\text{H}_2\text{PO}_4)_2^{2+}$ (Fuger, 1992). No other data was used due to the lack of characterization of the Pu phosphate solution species. The solubility product for $\text{PuPO}_4(\text{s})$, -21.5 ± 0.5 at 0.5 M NaClO_4 (Moskvin, 1971) was used and corrected to $\log K_{\text{sp}}^\circ = -24.6 \pm 0.5$.

Sulphates. The reported formation constants of PuSO_4^+ (Nair and Rao, 1967; Rao et al., 1978) were used to obtain, after averaging and application of S.I.T., $\log\beta_1^\circ = 1.9 \pm 0.6$. $\log\beta_1^\circ = 5.5 \pm 0.5$ and $\log\beta_2^\circ = 7.7 \pm 0.7$ were adopted for the formation of PuSO_4^{2+} and $\text{Pu}(\text{SO}_4)_2(\text{aq})$ (Fuger, 1992). The reported data for $\text{PuO}_2(\text{SO}_4)(\text{aq})$ scatter by about two orders of magnitude (Patil and Ramakrishna, 1976; Ullman and Schreiner, 1986), and the average, $\log\beta_1^\circ = 2.4 \pm 1.0$, was used as a first estimate.

Chlorides. Recent EXAFS studies showed that Pu(III) does not form inner-sphere complexes with chloride at Cl^- concentrations ≤ 14 M (Allen et al., 1997), but Pu–chloride complexes are known for Pu(IV) and Pu(VI). The recommended value for PuCl^{3+} , $\log\beta_1^\circ = 2.0 \pm 0.5$ (Fuger, 1992), was adopted but no consistent thermodynamic data for higher Pu(IV) chloro complexes exist. The thermodynamic data available for Pu(VI) chloro complexes are not in good agreement, and only $\log\beta_1^\circ = 0.23 \pm 0.03$ (Runde et al., 1999) is used.

Nitrates. The authors adopted $\log\beta_1^\circ = 2.6 \pm 0.5$ for $\text{Pu}(\text{NO}_3)_3^{3+}$ (Fuger, 1992). Thermodynamic constants for other complexes cannot be recommended due to lack of precise experimental data.

2.4.6. Plutonium solid phases

Reliable thermodynamic data on a solubility-controlling solid phase supported by spectroscopic characterization are crucial to geochemical modeling efforts because the solubility product of that solid primarily controls the upper concentration boundary of soluble Pu in aqueous systems.

Carbonates. No Pu(III) or Pu(V) solid carbonates have been studied. A mixed Pu(IV) hydroxy carbonate, $\text{Pu}(\text{OH})_2\text{CO}_3(\text{s})$, was postulated to interpret solubility data in carbonate containing media (Kim et al., 1983). Because there is no experimental characterization, the authors do not recommend any thermodynamic data for this compound. The only known stable solid Pu(VI) carbonate is $\text{PuO}_2\text{CO}_3(\text{s})$, which is isostructural to $\text{UO}_2\text{CO}_3(\text{s})$. The solubility product of $\text{PuO}_2\text{CO}_3(\text{s})$ was experimentally determined to be $\log K_{\text{sp}} = -13.0$ in 0.1 M NaCl (Neu et al., 1997a), and -14.0 in 0.1 M NaClO_4 (Robouch and Vitorge, 1987). After correction to zero ionic strength, using the S.I.T. parameters for the analogue $\text{U}(\text{VI})\text{--CO}_3^{2-}$ system, the solubility product was averaged to $\log K_{\text{sp}}^\circ = -14.3 \pm 0.5$. This value agrees well with that of $\text{UO}_2\text{CO}_3(\text{s})$, $\log K_{\text{sp}}^\circ = -14.47 \pm 0.04$ (Grenthe et al., 1992).

Oxides and hydroxides. Despite numerous studies, the phase diagram of Pu oxides/hydroxides is poorly understood, and experimental solubility data scatter widely. Probably the most relevant solid phases for environmental applications are $\text{Pu}(\text{OH})_3$, PuO_2 , $\text{PuO}_2 \cdot n\text{H}_2\text{O}$ or $\text{Pu}(\text{OH})_4$, PuO_2OH , and $\text{PuO}_2(\text{OH})_2$. In most solubility studies, the solid phases lack accurate characterization and identification. The solubility product of $\text{Pu}(\text{OH})_3$, $\log K_{\text{sp}}^\circ = -26.2 \pm 0.8$, is derived from the single solubility study in deionized water after application of the Pitzer equations (Felmy et al., 1989). This value agrees well with that of $\text{Am}(\text{OH})_3(\text{s})$, $\log K_{\text{sp}}^\circ = -25.0 \pm 0.6$, (Silva et al., 1995). The authors adopted $\log K_{\text{sp}}^\circ(\text{Am}(\text{OH})\text{CO}_3(\text{s})) = -21.2 \pm 1.4$ (Silva et al., 1995) and calculated $\Delta_f G_{298}^\circ(\text{Pu}(\text{OH})\text{CO}_3(\text{s})) = -1227.6 \pm 8.7$ using $\Delta_f G_{298}^\circ(\text{Pu}^{3+}) = -578.6 \pm 3.3$ kJ mol^{-1} (Fuger and Oetting, 1976). The solubilities of solid Pu(IV) oxide/hydroxide scatter within multiple orders of magnitude because of the difficulties of establishing Pu(IV) equilibrium, polymerization and disproportionation reactions, and the strong affinity of $\text{Pu}^{4+}(\text{aq})$ to sorb on surfaces. The authors averaged the ionic strength corrected solubility products of hydrated Pu(IV) oxide, $\text{PuO}_2 \cdot n\text{H}_2\text{O}$ or $\text{Pu}(\text{OH})_4$ ($\log K_{\text{sp}}^\circ = -58.4 \pm 0.3$ (Kasha, 1949), -59.4 ± 0.4 (Perez-Bustamante, 1965), -58.7 ± 0.3 (Rai, 1984), -57.9 ± 0.6 (Lierse and Kim, 1986), -58.0 ± 0.3 (Kim and Kanellakopoulos, 1989), and -58.3 ± 0.5 (Capdevila and Vitorge, 1998)), and obtained $\log K_{\text{sp}}^\circ = -58.5 \pm 1.0$. This value is in good agreement with the solubility product of amorphous Pu(IV) hydroxide, $\log K_{\text{sp}}^\circ = -58.7 \pm 0.9$ (Knopp et al., 1999). The reported value of the more crystalline $\text{PuO}_2(\text{s})$, $\log K_{\text{sp}}^\circ = -63.8 \pm 1.0$ (Kim and Kanellakopoulos, 1989) was adopted. The available data for $\text{PuO}_2\text{OH}(\text{s})$ ($\log K_{\text{sp}}^\circ = -8.6$ (Kraus and Nelson, 1948) and -9.3 (Zaitseva et al., 1968)) were averaged to obtain $\log K_{\text{sp}}^\circ = -8.9 \pm 0.3$, which is in good agreement with the solubility product for amorphous $\text{NpO}_2\text{OH}(\text{s})$, $\log K_{\text{sp}}^\circ = -8.77 \pm 0.09$ (Kaszuba and Runde, 1999). Data on the solubility of $\text{PuO}_2(\text{OH})_2(\text{s})$ appear to scatter by two orders of magnitude. The ionic strength corrected values of two studies ($\log K_{\text{sp}}^\circ = -21.7 \pm 0.1$ (Pashalidis et al., 1995) and -23.6 (Kim et al., 1983)) were averaged to give $\log K_{\text{sp}}^\circ = -22.7 \pm 1.0$. No thermodynamic data are available for the superoxide PuO_{2+x} .

3. Results and discussion

Assessment of radionuclide mobility requires knowledge of the chemical behavior of radionuclides in the infiltrating waters. The chemical conditions in the near-field may significantly alter when the water reacts with the waste package and/or backfill materials. Consequently, risk assessment calculations must cover radionuclide immobilization scenarios over a range of

chemical parameters (i.e. Eh, pH, and ionic strength). Geochemical modeling of radionuclide transport quantifies stabilities of radionuclide species in equilibrium or at steady state with each other in varying environments. For acceptable geochemical modeling, it is crucial that reliable thermodynamic data be available for the most important solution and solid state compounds. Experimental data obtained under site-specific conditions may be used to test the quality of the thermodynamic data-base.

The Eh–pH range of most natural waters (including J-13), that is pH 4–9 and Eh -0.2 to +0.6 V, overlaps with the stability fields of Pu(III), Pu(IV), Pu(V), and Pu(VI) (Fig. 1). The higher oxidation states, V and VI, are unstable in water as bare cations and undergo coordination by forming the linear dioxo-cations PuO_2^+ and PuO_2^{2+} , respectively. In carbonated water, Pu exhibits only one triple point ($\text{PuF}_2^{2+}/\text{PuO}_2^+/\text{PuO}_2\text{F}^+$) at a pH of 2.4 where species in the IV, V, and VI oxidation states are calculated to coexist at equilibrium. Plutonium(III) can occur only in natural waters at low redox potentials (below 300 mV at pH 5 and below 0 mV at pH 7). Tetravalent Pu, in the form of the tetrahydroxo complex, $\text{Pu}(\text{OH})_4(\text{aq})$, dominates the solution speciation in J-13 water (pH about 7, Eh about 430 mV (Efurud

et al., 1998)) and is the most stable solution species at pH values > 6. Increasingly oxidizing conditions favor the stability of plutonyl(V) and (VI) species. The PuO_2^+ ion and its monocarbonato complex, $\text{PuO}_2\text{CO}_3^-$, are the most important Pu(V) solution species under J-13 water conditions similar to the Np(V) system. Hydroxide complexation of Pu(V) is significant only at a pH above 13.5. Plutonium(VI) species reside within the water stability range at very high redox potentials, and carbonate complexation dominates hydrolysis. The stability fields of Pu(VI) species are small, and Pu(VI) is unlikely to persist in geochemical systems of low salinity. However, in the near environment of high-level nuclear waste, Pu(VI) may be formed by radiolysis. Among the minor ligands in J-13 water, only F^- affects the solution speciation of Pu. Fluoride complexes of Pu(IV) and Pu(VI) are calculated to exist at very low pH and redox potentials above 580 mV. Ultimately, depending on the Eh and pH of the infiltrating water after its interaction with the waste package materials, Pu(III), Pu(IV), and Pu(V) most likely control the transport characteristics of Pu.

Solid $\text{Pu}(\text{OH})_4(\text{s})$ is insoluble at pH values > 3 (the shaded area in Fig. 1 represents soluble Pu concentrations less than 10^{-5} M) and is calculated to be stable over Pu(III), Pu(IV), Pu(V), and Pu(VI) in solution. The

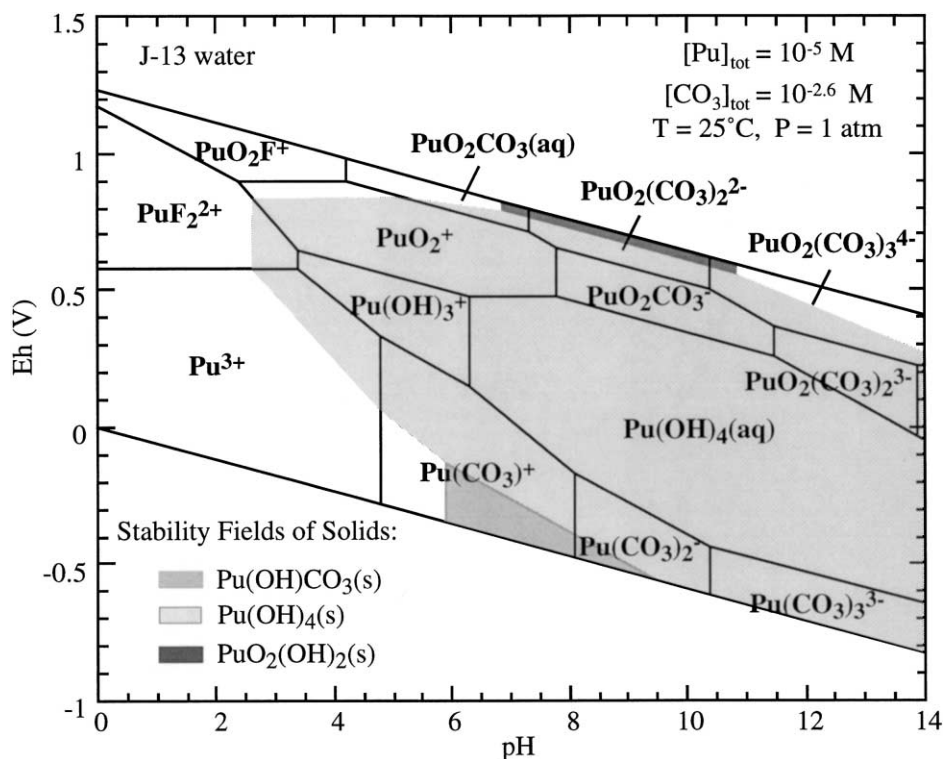


Fig. 1. Eh–pH diagram for Pu under J-13 water conditions at 25 °C. The diagram shows the stability fields of the predominant aqueous Pu species (solid lines). Boundaries of the relevant Pu solids that are oversaturated in 10^{-5} M Pu solutions are shown in the shaded areas. Formation of $\text{PuO}_2(\text{s})$ was suppressed.

thermodynamically more stable $\text{PuO}_2(\text{s})$ would cover almost the entire water stability field and precipitate from 10^{-5} M Pu solutions at pH values >1.3 . At extremely low and high redox potentials, $\text{Pu}(\text{OH})\text{CO}_3(\text{s})$ and $\text{PuO}_2(\text{OH})_2(\text{s})$, respectively are calculated to control Pu solubility in the near-neutral pH range. Under most conditions of natural waters, Pu(IV) solid phases are calculated to dominate and control overall Pu solubilities.

3.1. Solubility and speciation studies

The authors previously reported results of Pu and Np solubility studies in J-13 water (Efurud et al., 1998). At ambient temperature, Pu solubility decreased from 5×10^{-8} mol/l to 9×10^{-9} mol/l over the pH range from 6 to 8.5 (Fig. 2). Only a slight decrease in Pu solubility with increasing pH was observed at 60 °C. At 90 °C, the experimental Pu concentrations were pH-independent at 4×10^{-9} mol/l in the pH range 6–8. At a given pH, the soluble concentrations remained constant over a reaction time of about 400 days (except at pH of 7 at 25 °C). In all experiments, dark green precipitates were present and controlled the Pu solubility boundaries. X-ray diffraction and diffuse reflectance spectra indicated the presence of Pu(IV) in the solid phase (Efurud et al., 1998). The Bragg reflections of the Pu solids precipitated at ambient temperature were very broad and diffuse suggesting the presence of an amorphous Pu(IV) hydroxide or Pu(IV) colloid. The diffraction pattern of the 90 °C solid exhibited more distinct reflections indicating an increased crystallinity and higher-ordered solid. The diffraction pattern of all solids investigated showed signs of $\text{PuO}_2(\text{s})$ and the main reflections of the 90 °C solid can be assigned to the Fm3m $\text{PuO}_2(\text{s})$ phase (Mooney and Zachariasen, 1949). However, first spectroscopic investigations of the 90 °C precipitate dis-

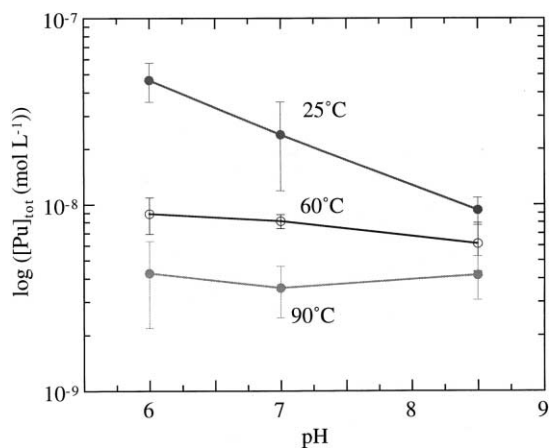
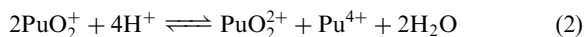


Fig. 2. Temperature dependence of the Pu solubility in J-13 water at pH values of 6, 7, and 8.5.

solved in 3 M HCl showed an absorbance peak at 830 nm characteristic of $\text{PuO}_2^{2+}(\text{aq})$ (Efurud et al., 1998). Although the observation of Pu(VI) indicated the presence of oxidized Pu in the solution phase, it cannot verify the presence of Pu(V) or Pu(VI) in the solid phase. Plutonium(V) is unstable in acidic solution, and its disproportionation reaction is fourth-power dependent on the H^+ concentration according to Eq. (2) (Choppin et al., 1997):



The appearance of oxidized Pu suggests the presence of the superoxide $\text{PuO}_{2+x}(\text{s})$ that was reported to contain Pu(VI) and was synthesized between 25 and 350 °C in humid conditions (Stakebake et al., 1993; Haschke and Ricketts, 1997; Haschke et al., 2000). Plutonium(VI) was identified by X-ray photoelectron spectroscopic (XPS) analysis to be present in small but different quantities at different temperatures. Recent XAS studies, however, revealed the existence of Pu(V) instead of Pu(VI) (Morales et al., in preparation). Fig. 3 shows the XAS spectrum (left), the raw k^3 -weighted EXAFS data (right top), and the corresponding phase-shift corrected Fourier Transform (right bottom) for the Pu solid precipitated at 90 °C in J-13 water compared with data for the $\text{PuO}_2(\text{s})$ standard. The XAS spectra of precipitate and standard were identical, and no significant differences in the k^3 -weighted EXAFS data were observed. A number of Pu–O distances were observed in the range of 2.3–3.7 Å for short and longer Pu–O distances characteristic of the Pu(IV) colloid (Neu et al., 1997b; Conradson, 1998). A reduced amplitude at 2.27 Å indicates only a small amount of short Pu–O distances

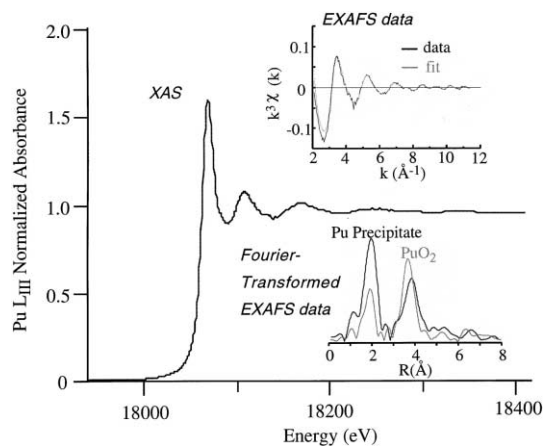


Fig. 3. XAS study of the Pu solid formed in J-13 water from oversaturation at 90 °C. The top right inset shows the background-corrected k^3 -weighted EXAFS data and the fit of these data. The right bottom inset compares the Fourier-transformed EXAFS data for the precipitate with the FT data for a standard $\text{PuO}_2(\text{s})$.

representative of presumably terminal Pu–OH moieties that are also observed in colloidal Pu(IV) materials (Neu et al., 1997b). The observed Pu–O distance of 2.27 Å, however, is shorter than the 2.33 Å for Pu–O in PuO₂(s) and oxo-bridges in colloidal Pu(IV) that range between 2.36 and 3.72 Å (Neu et al., 1997b; Conradson, 1998). The intense amplitude at 3.86 Å corresponds to Pu–Pu distances that are slightly longer than those in Pu(IV) colloid (3.84 Å) and PuO₂(s) (3.83 Å) (Neu et al., 1997b; Conradson, 1998).

The Fourier Transform (Fig. 3, right bottom) also indicated a Pu–O distance of about 1.85 Å, which is characteristic for the plutonyl distance in Pu(V) and agrees well with the plutonyl bond distance of 1.81 Å in the PuO₂⁺(aq) ion (Conradson, 1998). The Pu–O bonds in compounds of hexavalent Pu are generally much shorter, i.e. 1.74 Å in PuO₂²⁺(aq) (Conradson, 1998). However, the amount of this Pu(V) feature is sufficiently small so as not to affect the XANES spectra, which shows only the features of Pu(IV) (oxy)hydroxide. The inflection point in the XANES spectrum for Pu(V) compounds is at or slightly below that of Pu(IV), whereas Pu(VI) compounds exhibit substantially higher inflection points. The absence of such an inflection point shift in the XANES data is consistent with the presence of Pu(V) instead of Pu(VI). The plutonyl(V) bond distance of 1.85 Å has only been observed in the solid recovered from the high-temperature solubility experiment. At ambient temperature, oxidation of Pu(IV) is extremely slow and formation of Pu(V) was not observed after 400 days. Slow kinetics of Pu(V) formation were also reported when PuO₂(s) was reacted at 25 °C with adsorbed water, and the value of x in PuO_{2+x}(s) reached a value of only 0.003 in 4 years, whereas x achieved 0.17 at 350 °C (Haschke et al., 2000).

Based upon the understanding of Pu solid phase stabilities, the authors calculated the range of Pu solubilities in J-13 water at 25 °C spanned by variation in pH (3–10), Eh (0–600 mV), and total carbonate concentrations (0.1–2.8 mmolal). The solubility was calculated by introducing two solubility-controlling Pu(IV) solids, PuO₂(s) and Pu(OH)₄(s), and by allowing Pu(III), Pu(IV), Pu(V), and Pu(VI) to react in solution. The solid lines in Fig. 4 represent the calculated soluble Pu concentration limits over Pu(OH)₄(s) (Fig. 4 top) and PuO₂(s) (Fig. 4 bottom) at 0–600 mV in 100 mV increments. The shaded area confines the calculated soluble Pu concentration range spanned by Eh values between 0 and 600 mV and controlled by the presence of the corresponding solid Pu(IV) phase. The more crystalline PuO₂(s) is thermodynamically more stable than its amorphous hydration product Pu(OH)₄(s) (or PuO₂·2H₂O(s)), and Pu solubility is lowered by several orders of magnitude. Pure Pu(III), Pu(V), and Pu(VI) phases, such as oxides, hydroxides, or carbonates, are undersaturated in J-13 water and are not relevant for solid-liquid phase

equilibrium calculations. PuO₂(OH)₂(s) can exist as a solid phase only at unusually high values of Eh (> 550 mV) and pH (> 9) and in the absence of the poorly soluble PuO₂(s) (Fig. 4 top). Thus, in contrast to the analogous Np system in which Np₂O₅(s) and Np(IV) (oxy)hydroxide can exist in J-13 water, only the solid Pu(IV) phases, PuO₂(s) or Pu(OH)₄(s), affect Pu solubility.

The solubility of PuO₂(s) or Pu(OH)₄(s) remains within about two orders of magnitude if only Pu(IV) species are present in solution (bottom lines in Fig. 4). At pH values > 6, the soluble Pu(IV) concentration remains constant at 10⁻¹⁶ M (over PuO₂(s)) or 10⁻¹¹ M (over Pu(OH)₄(s)). Introducing other oxidation states by varying Eh causes significant changes in the solubility behavior. Under alkaline conditions, Pu solubility increases with Eh due to the formation of Pu(V) and Pu(VI) species and the increased concentration ratios [Pu(V)]:[Pu(IV)] and [Pu(VI)]:[Pu(IV)] in solution. At pH values below 7, Pu solubility increases with decreasing Eh caused by the successive stability of Pu(III) in solution. Within the Eh range of J-13 water in solubility and drip-test studies, 400–600 mV, overall Pu behavior is sensitive to small changes in redox potential that may cause crucial changes in oxidation state stability and solution speciation that affect transport characteristics. As illustrated in Fig. 5 (top), Pu(III) species define solution speciation at an Eh of 400 mV and pH values below pH 5, and [PuO₂CO₃⁻] increases above pH 8. In the pH range from 6 to 9, Pu(OH)₄(aq) remains the dominant solution species. Under J-13 water conditions (Eh about 430 mV and pH around 7), about 25% of the dissolved Pu exists as Pu(V). However, at 500 mV, the fraction of Pu(IV) solution species is reduced to about 25%, and both PuO₂⁺ and PuO₂CO₃⁻ are most important at pH > 6. In fact, carbonate complexes are the dominant Pu(V) solution species in J-13 water at pH above 8. At Eh values above 400 mV, those Pu(V) carbonate complexes increase the overall Pu solubility. A decrease in carbonate reduces the amount of Pu carbonate complexation and thus lowers the soluble fraction of Pu species under basic conditions. High pH and Eh stabilize Pu in the hexavalent oxidation state but Pu(VI) is not expected to be relevant under Yucca Mountain conditions.

The calculated solubilities are compared in Fig. 4 with experimental data from solubility experiments (Nitsche et al., 1993; Efurud et al., 1998) and dissolution data of spent nuclear fuel (Finch et al., 1999; CRWMS, 2000). The drip tests at 90 °C simulate the unsaturated and oxidizing conditions expected at Yucca Mountain and provide information on the long-term dissolution and release rate of spent nuclear fuel. J-13 water was injected at drip rates of 0.15 and 1.5 ml per week (Finn et al., 1996a, b; Finch et al., 1999; CRWMS, 2000). Based on the release and the Eh-pH diagrams of Tc, Mo, Ru, Rh,

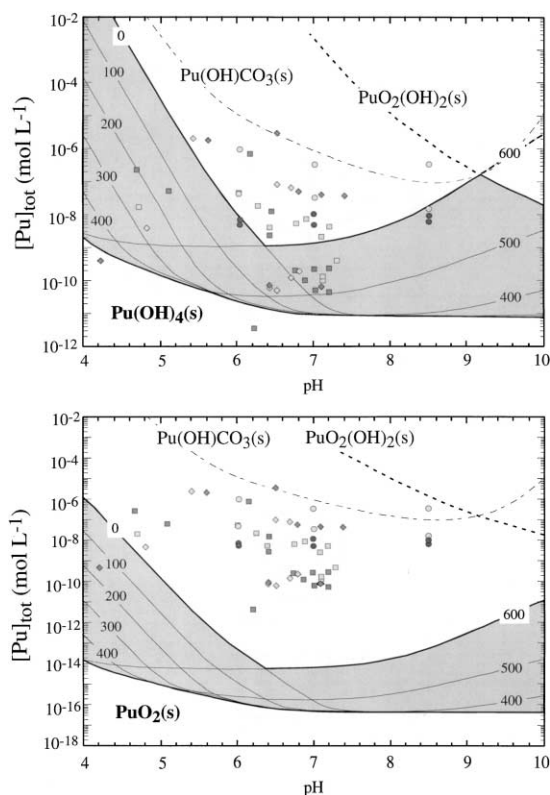


Fig. 4. Calculated solubilities of Pu in J-13 water at 25 °C and various Eh values. The solid lines are calculated Pu solubilities for the individual Eh values given in mV. The shaded area represents overall Pu solubilities between 0 and 600 mV over $\text{Pu}(\text{OH})_4(\text{s})$ (top) and $\text{PuO}_2(\text{s})$ (bottom). Changes in soluble concentrations with Eh are due to the variable stabilities of Pu(III), (V), and (VI) species in solution. Plutonium concentrations below the lowest solubility boundary are not controlled by a solid–liquid phase equilibrium. The solubility data from oversaturation experiments (\bullet from Efurd et al., 1998; \circ from Nitsche et al., 1993) and the concentrations in J-13 water from high-flow (\blacklozenge) and low-flow (\diamond) drip-tests (Finn et al., 1996a,b; Finch et al., 1999; CRWMS, 2000) are shown for comparison.

and Pd, the oxidation potential at the fuel surface was estimated to be as high as +600 mV (Finn et al., 1996b). The calculated solubility of the crystalline phase $\text{PuO}_2(\text{s})$ is lower by several orders of magnitude than all reported experimental data. Approximately 50% of the drip-test data overlap with calculated Pu solubilities at near-neutral pH and Eh values between 500 and 550 mV (about 10^{-10} mol/L Pu), whereas the remaining data are scattered above calculated solubility levels. Data from oversaturation solubility experiments are about two orders of magnitude higher than calculated. Considering the results from XAS investigations of the Pu(IV) solid, increased Pu concentrations are presumably caused by the generation of intrinsic Pu(IV) colloids that are

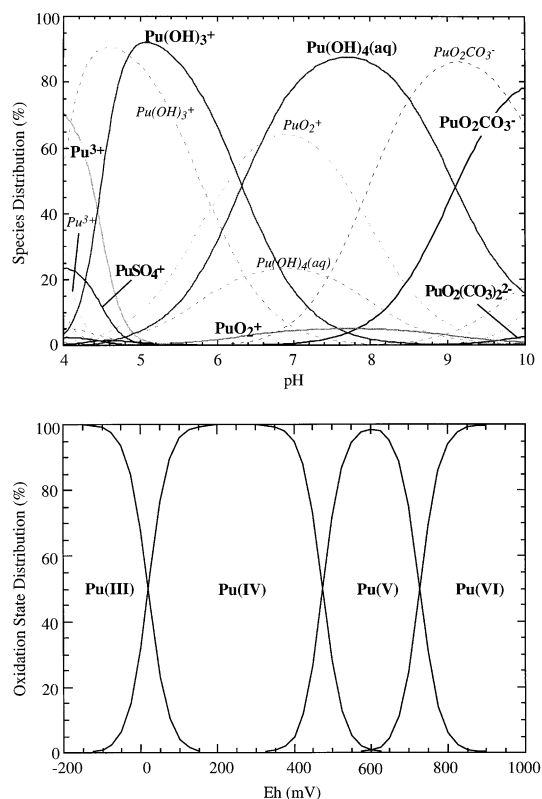


Fig. 5. Speciation of Pu in J-13 water at 25 °C: The top panel shows the species distribution at an Eh of 400 mV (solid lines) and 500 mV (dashed lines) as a function of pH. The bottom graph shows the calculated stabilities of Pu(III), (IV), (V), and (VI) as a function of Eh at a pH of 7 and 2.8 mmol total carbonate.

known to stabilize Pu in solution. These intrinsic colloids span a wide range of structural features, crystallinities, and stabilities and are known to increase soluble Pu significantly (Capdevila and Vitorge, 1998; Knopp et al., 1999). The discrepancies within the data of oversaturation solubility studies were explained by the different amounts of colloidal Pu(IV) species present in the experiments (Efurd et al., 1998). It should be noted, that experimental data are obtained within a temperature range of 25–90 °C whereas the thermodynamic database is limited to 25 °C. Plutonium speciation and solubilities may change substantially within this temperature range. Equilibrium constants for reactions at high temperature can be calculated from $\Delta_r G^\circ$ and $\Delta_r S^\circ$ at 25 °C and the heat capacity change $\Delta_r C_p$ for the reaction over the corresponding temperature range. However, data for $\Delta_r S^\circ$ and $\Delta_r C_p$ are not available for most environmentally relevant reactions of Pu species and modeling of Pu speciation and solubility at high temperatures remains highly uncertain.

3.2. Sorption studies

The precipitation of a secondary radionuclide-bearing solid may be a reasonable approximation of upper boundaries of soluble radionuclide at slow infiltration rates of water into the repository. Saturation of the aqueous phase with radionuclides depends on various parameters, such as composition and infiltration rate of the water or the kinetics of waste dissolution. In many scenarios, however, dissolved Pu and Np concentrations remain below saturation and most likely undergo interactions at the solid–solution interfaces of waste package materials, soils, and minerals. Specifically, the extent of radionuclide interaction with colloidal matter is critical because the pseudocolloids formed can be mobile and enhance the transport of strongly sorbing radionuclides along flow paths to the accessible environment.

Slow degradation of waste packages is expected to occur within the first 10ka of repository closure producing alteration phases and several types of colloidal material. Natural groundwater colloids exist in almost all subsurface environments and result from the weathering of geological and biological materials. Composition, stability, and concentration of natural colloids differ from one groundwater to another and depend on the chemical and physical steady state in the hydro-geochemical system (Degueldre et al., 2000). It is assumed that because of the presence of Ca in Yucca Mountain aquifers, the complexation capacity of natural organic colloids, i.e. humics, is reduced and insignificant for radionuclide transport calculations (Minai et al., 1992). Iron(oxy)hydroxide may be produced by corrosion of the Fe-based waste package steels. Dissolution of high-level waste glass and spent nuclear fuel may generate clay (mainly smectite) and silica colloidal material (CRWMS, 2000). These colloids generally have composition and surface characteristics similar to the immobile aquifer solids but are mobile within the aquifer. The large surface area of these colloids (10^4 – 10^5 m²/kg) offers significant sorption capacities for radionuclides. The sorption processes that control adsorption of radionuclides to minerals and soil also affect their association with colloidal materials with similar functional groups.

Batch sorption experiments were performed from undersaturated solutions with respect to pure solid Pu and Np phases selecting hematite, montmorillonite, and silica particles as the most important colloid types for the Yucca Mountain site. As expected for pentavalent actinide ions, uptake of Np on the different types of colloids was low, and generally less than 15% of the total dissolved Np species were removed from solution (Fig. 3). Accordingly, the sorption distribution coefficients were low: 880 ml/g for hematite, 150 ml/g for montmorillonite, and 550 ml/g for silica after 240 hours

reaction time. In all experiments, the majority of Np (over 80%) remained in solution as molecular species. The K_d values for Np(V) uptake on montmorillonite are close to the bulk of the reported values ranging between 10 and 100 ml/g (Turner et al., 1998). Crystalline quartz on the other hand is reported to not sorb Np(V) in significant amounts up to a pH of 9 (Kohler et al., 1999), and less than 20% of total dissolved Np could be sorbed on amorphous silica at a pH of 8 (Righetto et al., 1991). The extent of Np(V) uptake depends on the pH, the carbonate concentration, and the amount and the crystallinity of the mineral introduced (Nakayama and Sakamoto, 1991; Sakamoto et al., 1994; Tochiyama et al., 1995; Kohler et al., 1999). At given conditions, sorption at a pH of 8 may vary between 95% and less than 10% when the solid/liquid ratio is changed from 1 to 0.01 g/l (Nakayama and Sakamoto, 1991; Kohler et al., 1999). The low sorption of Np(V) on hematite observed in this study agrees well, considering the relatively low hematite colloid concentration of 0.2 g/l. A detailed comparison between uptake mechanisms and K_d values is difficult because of the use of several different types of clay, different mass/volume ratios, and the lack of spectroscopic characterization of surface complexes.

Uptake of Pu(V) decreased from hematite to silica and montmorillonite with fast sorption kinetics followed by a subsequent, gradually increasing, Pu uptake with time (Fig. 6). As for other heavy metals, Fe(III) (oxy)hydroxides are an effective sink for the uptake of Pu. Hematite sorbed Pu irreversibly within hours with about 95% Pu uptake occurring within the first 48 h of contact time. The K_d value ranged between 4.9×10^3 and 1.8×10^5 ml/g. An even slightly faster uptake of Pu within the first hour followed by a gradual increase was also observed with goethite, α -FeOOH (Sanchez et al., 1985). Hematite generally exhibits lower sorption capacities for multivalent cations than goethite and correlates well with the pH-dependent sorption of other oxides of similar structure, such as alumina α -Al₂O₃ (Nakayama and Sakamoto, 1991). The higher and more rapid Pu uptake by goethite results from the differences in crystalline forms and mineral surface properties (Tochiyama et al., 1995; Kohler et al., 1999). The uptake capacity of montmorillonite and silica are significantly lower for both Pu and Np. Only between 50 and 60% of the Pu is sorbed after 240 hours and K_d values were similar, 5.8×10^3 ml/g for montmorillonite and 8.1×10^3 ml/g for silica. Again, fast sorption kinetics were observed within the first 100 hours with a subsequent gradual increase of sorbed Pu. The distribution coefficients measured at 200 mg/l colloid concentration increased slightly (between 2 and 4 times) when lowering the colloid concentrations to 10 mg/l. Thus, the concentration of sorbed Pu was higher in colloid-poor water than in the presence of higher amounts of particulates

where colloid aggregation may contribute to the reduction of available surface area per unit mass of colloids.

In all experiments Pu(V) reacted far stronger with the colloidal surfaces than its chemical analogue Np(V). Because Np(V) and Pu(V) generally behave chemically similar in solution, the higher uptake of Pu indicates a more complex interaction mechanism. In the absence of colloids, Pu(V) and Np(V) were stable in solution, and the soluble Pu concentration did not decrease due to reduction of Pu(V) to the less soluble Pu(OH)₄(aq). Reduction of Pu(V) agrees with the reported shift of Pu adsorption with time, approaching the colloidal uptake curve of Pu(IV) (Sanchez et al., 1985). Keeney-Kennicut and Morse (1985) reported the disproportionation reaction of PuO₂⁺ on goethite to form Pu(IV) and Pu(VI). The latter is slowly reduced to Pu(IV), leaving Pu(IV) as the dominant surface species. Different uptake kinetics were also observed for Np(IV) and Np(V) interaction with marine particulates (McCubbin and Leonard, 1997). Neptunium(IV) exhibits a rapid initial sorption followed by desorption over long period of time, whereas the uptake of Np(V) remained below 20% and occurred at a much slower rate. Consequently, reductive processes at the mineral–water interface most likely contribute to the high uptake of Pu(V), and reported K_d values represent uptake of Pu(IV) rather than Pu(V).

Increasing the temperature from 20 to 80 °C increased the uptake of Np on montmorillonite, hematite, and silica by up to 20% and increased the K_d values by up to one order of magnitude (Figs. 7). With the exception of montmorillonite, temperature did not affect the uptake of Pu as significant as for Np; however, a general trend of increased uptake of Pu(V) with temperature was observed. Although sorption on hematite and silica increased only up to 7%, Pu uptake on montmorillonite increased by about 38% as temperature increases from 20 to 80 °C. It has to be determined whether increased activity of the surface sites or changing redox stability and complexation behavior of the actinides in solution caused the increased uptake of Pu and Np.

Little information is available on the reversibility of actinide sorption and the stability of pseudocolloids along a transport pathway. Desorption of Pu and Np from hematite, montmorillonite, and silica pseudocolloids was studied in fresh natural water from well J-13. The low levels of uptake of Np prohibited the reliable monitoring of the concentration of released Np over time. Desorption of Pu was considerably slower than the adsorption process. As expected, hematite sorbed Pu very strongly, and only minor amounts of Pu (less than 1%) desorbed after 290 days. This fact agrees well with low desorption of Pu from goethite after 30 days (Keeney-Kennicut and Morse, 1985). On the other hand, montmorillonite and silica released up to 21% of the adsorbed Pu upon contact with fresh J-13 water.

Consequently, the high stability of hematite pseudocolloids may be the primary facilitator of long-distance transport of actinides to the accessible environment. The low sorption of Np suggests that the main transport in aerobic waters will be as a dissolved solution species and also confirms the prime importance of this radionuclide for nuclear waste repository risk assessment.

4. Concluding remarks

Plutonium solubility in J-13 water is controlled by Pu(IV) solid phases only. Although crystalline PuO₂(s) is calculated to be the thermodynamic most stable solid phase, a more amorphous/colloidal Pu(IV) phase is kinetically favored and persisted in solubility experiments at ambient temperature over 400 days. Geochemical modeling using existing thermodynamic data results in about two orders of magnitude lower Pu concentrations than is observed, suggesting inaccuracies in the database or the formation of colloidal Pu(IV) species. In fact, the formation and well-known stability of intrinsic Pu(IV) colloids are not considered in any thermodynamic database available. High temperature increased the crystalline character of the solid phase and lowered the Pu solubility. However, it also led to the radiolytic formation of the superoxide PuO_{2+x}(s) that may be the cause of a slight increase in Pu solubility observed at 90 °C after about 250 days. Although this increase is rather insignificant within the 400 days of investigation, over longer time spans, it might lead to the formation of a solid Pu phase with higher solubility.

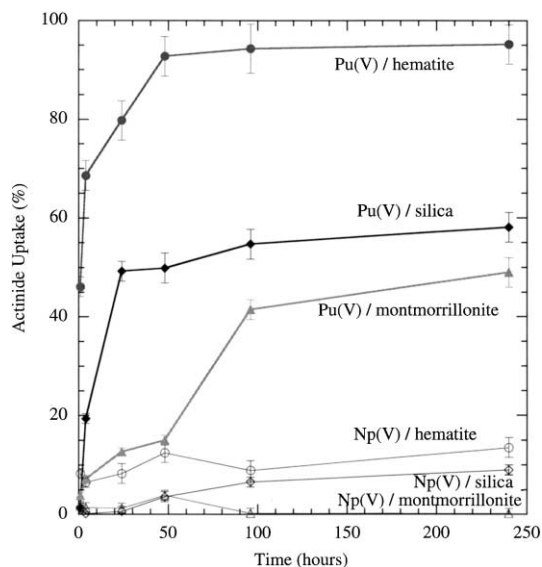


Fig. 6. Uptake of Np(V) and Pu(V) on hematite, montmorillonite, and silica colloids in J-13 water as a function of time at 25 °C and colloidal concentrations of 200 mg/l.

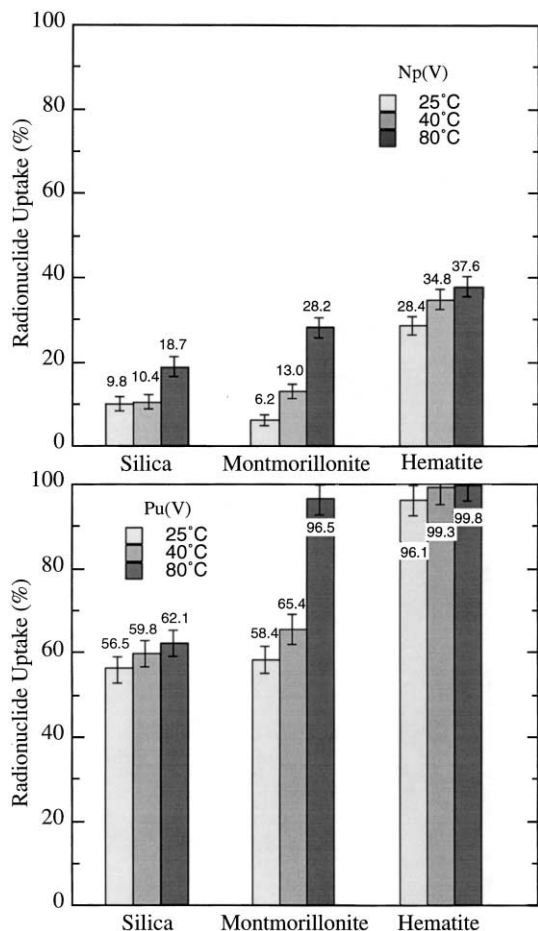


Fig. 7. Uptake of Np(V) (top) and Pu(V) (bottom) on hematite, montmorillonite, and silica colloids in J-13 water at 25, 40 and 80 °C (after 10 days of sorption).

Dissolution of $\text{PuO}_{2+x}(\text{s})$ may release Pu(V) which is more mobile than the less-soluble Pu(IV) (in the form of $\text{Pu}(\text{OH})_4(\text{aq})$ at neutral pH). The stability of Pu(V) in the solution phase, however, is mainly controlled by the Eh and pH of its system and the kinetics of the disproportionation reaction. More oxidizing conditions favor the persistence of Pu(V), and together with the formation of $\text{PuO}_{2+x}(\text{s})$, overall Pu solubility will increase. Under reducing conditions, Pu(V) is reduced to Pu(IV) and, thus, oxidation state impurities in $\text{PuO}_{2+x}(\text{s})$ will not significantly affect overall Pu solubility. While $\text{PuO}_{2+x}(\text{s})$ may liberate Pu(V) (or Pu(VI)) on dissolution, the overall stability of solution species will depend only on the Eh value of the solution and not on the nature of the solid phase. It should be noted that all these calculations are based on thermodynamic equilibria between the compounds. The proposed presence of Pu(VI) in the solid phase and its proposed effect on Pu mobility (Haschke et al., 2000) under Yucca Mountain conditions could not be verified in this study.

Reactions at the water–solid surfaces tend to differ significantly because of the higher redox reactivity of Pu. Uptake of Pu generally is higher than observed for Np under comparable conditions and is much less dependent on pH and carbonate relative to the Np(V) system because of the formation of the $\text{NpO}_2\text{CO}_3^-$ complex at above neutral pH. Differences in uptake kinetics suggest a reductive uptake mechanism with formation of Pu(IV) complexes on the mineral surface. Because Pu(V) is stable in the control experiments in which the sorbent is absent, Pu uptake depends strongly on the Pu(V)/Pu(IV) redox couple. The redox potentials for the Pu(V)/Pu(IV) and Np(V)/Np(IV) couples at neutral pH are reported to be +700 and +150 mV, respectively (Choppin, 1983). These data indicate that the reduction of Pu(V) to Pu(IV) needs less reducing conditions and that Pu(IV) can exist to some extent in solutions under ambient conditions. An electrostatic double layer on a mineral surface may alter the actinide's bulk properties by changing species activities (Turner et al., 1998). The fact that the reduction of Pu(V) to Pu(IV) is favored over the reduction of Np(V) to Np(IV) is reflected in the much slower increase of Np uptake with time.

The transport behavior of Pu in the far-field of the repository is strongly affected by the reversibility of the sorption process onto colloidal matter. Plutonium is stabilized by iron (oxy)hydroxides and may be transported over long distances. Silica and montmorillonite release adsorbed Pu in a new environment to a significant amount, thus changing the transport mechanism in a water flow. Resuspension of Pu allows the Pu to undergo successive geochemical reactions, such as complexation in solution, redox reactions, or interaction with mineral surfaces or other groundwater particulates. As a result, Pu may accumulate in the far-field of a repository. To model the migration of Pu and Np from a repository, various cooperative processes, including solubility and speciation, reactions at the mineral–water interface, and colloid formation and stability, all dependent on water composition, must be taken into account. Advanced spectroscopic techniques may help to further quantify the stepwise interaction mechanisms of redox-sensitive radionuclides with naturally abundant surfaces.

Acknowledgements

This work was supported by the Yucca Mountain Site Characterization Project Office of Los Alamos National Laboratory as part of the Civilian Radioactive Waste Management Program of the US Department of Energy. The authors would like to thank Drs. R. J. Finch, M. P. Neu, J. P. Kaszuba, R. C. Eckhardt, and D. K. Hyer for helpful discussions.

References

- Allen, P.G., Bucher, J.J., Shuh, D.K., Edelstein, N.M., Reich, T., 1997. Investigation of aquo and chloro complexes of UO_2^{2+} , NpO_2^{2+} , Np^{4+} , and Pu^{3+} by X-ray absorption fine structure spectroscopy. *Inorg. Chem.* 36, 4676–4683.
- Ankudinov, A.L., Rehr, J.J., 1997. Relativistic calculations of spin-dependent X-ray absorption spectra. *Phys. Rev. B* 56, R1712–R1716.
- Bagawde, S.V., Ramakrishna, V.V., Patil, S.K., 1976. Complexing of tetravalent plutonium in aqueous solutions. *J. Inorg. Nucl. Chem.* 38, 1339–1345.
- Bennett, D.A., Hoffman, D., Nitsche, H., Russo, R.E., Torres, R.A., Baisden, P.A., Andrews, J.E., Palmer, C.E.A., Silva, R.J., 1992. Hydrolysis and carbonate complexation of dioxoplutonium(V). *Radiochim. Acta* 56, 15–19.
- Bethke, C. R., 1998. The Geochemist's Workbench Release 3.0. University of Illinois at Urbana-Champaign.
- Cantrell, K.J., 1988. Actinide(III) carbonate complexation. *Polyhedron* 7, 573–574.
- Capdevila, H., Vitorge, P., 1995. Redox potentials of $\text{PuO}_2^{2+}/\text{PuO}_2^+$ and $\text{Pu}^{4+}/\text{Pu}^{3+}$ at different ionic strengths and temperatures. Entropy and heat capacity. *Radiochim. Acta* 68, 51–62.
- Capdevila, H., Vitorge, P., 1998. Solubility product of $\text{Pu}(\text{OH})_4(\text{am})$. *Radiochim. Acta* 82, 11–16.
- Capdevila, H., Vitorge, P., Giffaut, E., 1992. Stability of pentavalent plutonium: spectrophotometric study of PuO_2^+ and Pu^{4+} disproportionation in perchloric media. *Radiochim. Acta* 58–59, 45–52.
- Capdevila, H., Vitorge, P., Giffaut, E., Delmau, L., 1996. Spectrophotometric study of the dissociation of the $\text{Pu}(\text{IV})$ carbonate limiting complex. *Radiochim. Acta* 74, 93–98.
- Carter, D.L., Mortland, M.M., Kemper, W.D., 1986. Specific surface. In: Klute, A. (Ed.), *Methods of Soil Analysis. Part 1—Physical and Mineralogical Methods*, Vol. Series: 5. American Society of Agronomy, Madison, WI, pp. 413–423.
- Choppin, G.R., 1983. Actinide solution chemistry. *Radiochim. Acta* 32, 43–53.
- Choppin, G.R., Rao, L.F., 1984. Complexation of pentavalent and hexavalent actinides by fluoride. *Radiochim. Acta* 37, 143–146.
- Choppin, G.R., Bond, A.H., Hromadka, P.M., 1997. Redox speciation of plutonium. *J. Radioanal. Nucl. Chem.* 219, 203–210.
- Cleveland, J.M., 1979. The chemistry of Plutonium. American Nuclear Society, La Grange Park, Illinois.
- Conradson, S.D., 1998. Application of X-ray absorption fine structure spectroscopy to materials and environmental science. *Appl. Spectros.* 52 (7), 252A–279A.
- Craig, P.P., 1999. High-level nuclear waste: the status of Yucca Mountain. *Annual Rev. Energy Environ.* 24, 461–486.
- CRWMS M&O, 2000. Commercial Spent Nuclear Fuel Degradation in Unsaturated Drip Tests. Input Transmittal WP-WP-99432.T, Las Vegas, Nevada, ACC: MOL. 20000 107.0209.
- Degueldre, C., Triay, I.R., Kim, J.I., Vilks, P., Laaksoharju, M., Miekeley, N., 2000. Groundwater colloid properties: a global approach. *Appl. Geochem.* 15, 1043–1051.
- DOE (US Department of Energy), 1988. Site Characterization Plan: Yucca Mountain Site, Nevada. Research and Development Area, Nevada. Office of Civilian Radioactive Waste Management, Washington, DC.
- Dozol, M., Hagemann, R., Hoffman, D.C., Adloff, J.P., Von-Gunten, H.R., Foos, J., Kasprzak, K.S., Liu, Y.F., Zvara, I., Ache, H.J., Das, H.A., Hagemann, R.J.C., Herrmann, G., Karol, P., Maenhaut, W., Nakahara, H., Sakanoue, M., Tetlow, J.A., Baro, G.B., Fardy, J.J., Benes, P., Roessler, K., Roth, E., Burger, K., Steinnes, E., Kostanski, M.J., Peisach, M., Liljenzin, J.O., Aras, N.K., Myasoedov, B.F., Holden, N.E., 1993. Radionuclide migration in groundwaters: review of the behaviour of actinides. *Pure Appl. Chem.* 65, 1081–1102.
- Efurd, D.W., Runde, W., Banar, J.C., Janecky, D.R., Kaszuba, J.P., Palmer, P.D., Roensch, F.R., Tait, C.D., 1998. Neptunium and plutonium solubilities in a Yucca Mountain groundwater. *Environ. Sci. Technol.* 32, 3893–3900.
- Fanghänel, T., Könnecke, T., Weger, K., Paviet-Hartmann, P., Neck, V., Kim, J.I., 1999. Thermodynamics of Cm(III) in concentrated salt solutions: carbonate complexation in NaCl solution at 25 °C. *J. Solut. Chem.* 28, 447–462.
- Felmy, A.R., Rai, D., Schramke, J.A., Ryan, J.L., 1989. The solubility of plutonium hydroxide in dilute solution and in high-ionic-strength chloride brines. *Radiochim. Acta* 48, 29–35.
- Finch, R.J., Buck, E.C., Finn, P.A., Bates, J.K., 1999. Oxidative corrosion of spent UO_2 fuel in vapor and dripping groundwater at 90 °C. Scientific Basis for Nuclear Waste Management XXII, Materials Research Society Symposium Proceedings, eds. D.J. Wronkiewicz and J.H. Lee, Vol. 556, 431–438.
- Finn, P.A., Hoh, J.C., Wolf, S.F., Slater, S.A., Bates, J.K., 1996a. The release of uranium, plutonium, cesium, strontium, technetium, and iodine from spent fuel under unsaturated conditions. *Radiochim. Acta* 75, 65–71.
- Finn, P.A., Hoh, J.C., Wolf, S.F., Surchik, M.T., Buck, E.C., Bates, J.K., 1996b. Spent fuel reaction: the behavior of the e-phase over 3.1 years. Scientific Basis for Nuclear Waste Management XX, Materials Research Society Symposium Proceedings, eds. W.J. Gray and I.R. Triay, Vol. 465, 527–534.
- Fuger, J., 1972. Thermodynamic properties of simple actinide compounds. In: Bagnall, K.W. (Ed.), *Lanthanides and Actinides*. Butterworths, London, Great Britain, pp. 157–210.
- Fuger, J., 1992. Thermodynamic Properties of actinide aqueous species relevant to geochemical problems. *Radiochim. Acta* 58/59, 81–91.
- Fuger, J.F., Oetting, F.L., 1976. The Chemical Thermodynamics of Actinide Elements and Compounds. Part 2: The Actinide Aqueous Ions. International Atomic Energy Agency.
- Grenthe, I., Fuger, J., Konings, R.J.M., Lemire, R.J., Muller, A.B., Nguyen-Trung, C., Wanner, H., 1992. *Chemical Thermodynamics of Uranium*. Elsevier Science Publishers B.V., New York.
- Harrar, J.E., Carley, J.F., Isherwood, W.F., Raber, E., 1990. Report of the Committee to Review the Use of J-13 Well Water in Nevada Nuclear Waste Storage Investigations.
- Haschke, J.M., Ricketts, T.E., 1997. Adsorption of water on plutonium dioxide. *J. Alloys Compounds* 252, 148–156.
- Haschke, J.M., Allen, T.H., Morales, L.A., 2000. Reaction of plutonium dioxide with water: formation and properties of PuO_{2+x} . *Science* 287, 285–287.

- Kasha, M., 1949. Reactions between plutonium ions in perchloric acid solution: rates, mechanisms, and equilibria. In: Seaborg, G.T., Katz, J.J., Manning, W.M. (Eds.), *The Transuranium Elements*, Research Papers. McGraw-Hill, New York, pp. 295–334.
- Kaszuba, J.P., Runde, W., 1999. The aqueous geochemistry of Np: dynamic control of soluble concentrations with applications to nuclear waste disposal. *Environ. Sci. Technol.* 33, 4427–4433.
- Katz, J.J., Seaborg, G.T., Morse, L.R., 1986. *The chemistry of the actinide elements*, 2nd ed.. Chapman Hall, London.
- Keeney-Kennicutt, W.L., Morse, J.W., 1985. The redox chemistry of Pu(V)O_2^+ interaction with common mineral surfaces in dilute solutions and seawater. *Geochim. Cosmochim. Acta* 49, 2577–2588.
- Kim, J.I., Kanellakopoulos, B., 1989. Solubility products of plutonium(IV) oxide and hydroxide. *Radiochim. Acta* 48, 145–150.
- Kim, J.I., Lierse, C., Baumgärtner, F., 1983. Complexation of the plutonium(IV) ion in carbonate-bicarbonate solutions. In: Carnall, W.T., Choppin, G.R. (Eds.), *ACS Symposium Series*. American Chemical Society, Washington DC, pp. 317–334.
- Knopp, R., Neck, V., Kim, J.I., 1999. Solubility, hydrolysis and colloid formation of plutonium(IV). *Radiochim. Acta* 86, 101–108.
- Kohler, M., Honeyman, B.D., Leckie, J.O., 1999. Neptunium(V) sorption on hematite ($\alpha\text{-Fe}_2\text{O}_3$) in aqueous suspension: the effect of CO_2 . *Radiochim. Acta* 85, 33–48.
- Kraus, K.A., Nelson, F., 1948. *The Hydrolytic Behavior of Uranium and the Transuranic Elements*. Report AECD-1864, Oak Ridge National Laboratory.
- Kraus, K.A., Dam, J.R., 1949. *The Transuranium Elements*. In: Seaborg, G.T., Katz, J.J., Manning, W.M.. McGraw-Hill, New York, pp. 466–499. 528–549.
- Krylov, V.N., Komarov, E.V., 1969. Investigation of the complex formation of Pu(IV) with the fluoride ion in solutions of HClO_4 by the ion-exchange method. *Soviet Radiochem.* 11, 94–96.
- Lemire, R.J., Tremaine, P.R., 1980. Uranium and plutonium equilibria in aqueous solutions to 200 °C. *J. Chem. Eng. Data* 25, 361–370.
- Lemire, R.J., Garisto, F., 1989. *The Solubility of U, Np, Pu, Th and Tc in a Geological Disposal Vault for Used Nuclear Fuel*. Atomic Energy of Canada Limited, Report AECL-10009, Whitehall Nuclear Research Establishment, Pinawa, Manitoba R0E 1L0.
- Lierse, C., Kim, J.I., 1986. *Chemisches Verhalten von Plutonium in Natürlichen Aquatischen Systemen: Hydrolyse, Carbonatkomplexierung und Redoxreaktionen*. Report RCM-02286, Technische Universität München. Institut für Radiochemie, Germany.
- McCubbin, D., Leonard, K.S., 1997. Laboratory studies to investigate short-term oxidation and sorption behavior of Np in artificial and natural seawater Solutions. *Mar. Chem.* 56, 107–121.
- Metivier, H., Guillaumont, R., 1972. Hydrolyse du plutonium tetravalent. *Radiochim. Radioanal. Lett.* 10, 27–35.
- Metivier, H., Guillaumont, R., 1976. Hydrolysis and complexing of tetravalent plutonium. *J. Inorg. Nucl. Chem., Supp.* 179–183.
- Minai, Y., Choppin, G.R., Sisson, D.H., 1992. Humic material in well water from the Nevada test site. *Radiochim. Acta* 56, 195–199.
- Mooney, R.C., Zachariasen, W.H., 1949. *The Transuranium Elements*, Part II. McGraw-Hill, New York.
- Morales, L.A., Conradson, S.D. and Haschke, J.M. (in preparation).
- Moskvin, A.I., 1971. Investigation of the complex formation of trivalent plutonium, americium, and curium in phosphate solutions. *Soviet Radiochem.* 13, 688–693.
- Nair, G.M., Rao, C.L., 1967. Study of plutonium(III)-sulphate complexes. *Radiochim. Acta* 7, 77–80.
- Nakayama, S., Sakamoto, Y., 1991. Sorption of Np on naturally-occurring iron-containing minerals. *Radiochim. Acta* 52/53, 153–157.
- Nash, K.L., Cleveland, J.M., 1994. The thermodynamics of plutonium(IV) complexation by fluoride and its effect on plutonium(IV) speciation in natural waters. *Radiochim. Acta* 36, 129–134.
- Neu, M.P., Reilly, S.D., Runde, W.H., 1997a. Plutonium solubility and speciation to be applied to the separation of hydrothermal waste treatment effluent. *Mat. Res. Soc. Symp. Proc. Scientific Basis for Nuclear Waste Management XX* 465, 759–765.
- Neu, M.P., Schulze, R.K., Conradson, S.D., Farr, J.D., Haire, R.G., 1997b. Polymeric plutonium(IV) hydroxide: formation, prevalence, and structural and physical characteristics. *Pu FUTURES- The Science* 89–90.
- Nitsche, H., Silva, R.J., 1996. Investigation of the carbonate complexation of Pu(IV) in aqueous solution. *Radiochim. Acta* 72, 65–72.
- Nitsche, H., Muller, A., Standifer, E.M., Deinhammer, R.S., Becraft, K., Prussin, T., Gatti, R.C., 1992. Dependence of actinide solubility and speciation on carbonate concentration and ionic strength in groundwater. *Radiochim. Acta* 58/59, 27–32.
- Nitsche, H., Gatti, R.C., Standifer, E.M., Lee, S.C., Muller, A., Prussin, T., Deinhammer, R.S., Maurer, H., Becraft, K., Leung, S., Carpenter, S.A., 1993. Measured Solubilities and Speciations of Neptunium, Plutonium, and Americium in a Typical Groundwater (J-13) from the Yucca Mountain Region. Report LA-12562-MS, Los Alamos National Laboratory.
- Pashalidis, I., Kim, J.I., Ashida, T., Grenthe, I., 1995. Spectroscopic study of the hydrolysis of PuO_2^{2+} in aqueous solution. *Radiochim. Acta* 68, 99–104.
- Pashalidis, I., Czerwinski, K.R., Fanghänel, T., Kim, J.I., 1997. Solid-liquid phase equilibria of Pu(VI) and U(VI) in aqueous carbonate systems. Determination of stability constants. *Radiochim. Acta* 76, 55–62.
- Patil, S.K., Ramakrishna, V.V., 1976. Sulphate and fluoride complexing of U(VI), Np(VI), and Pu(VI). *Inorg. Chem.* 38, 1075–1078.
- Perez-Bustamente, J.A., 1965. Solubility product of tetravalent plutonium hydroxide and study of the amphoteric character of hexavalent plutonium hydroxide. *Radiochim. Acta* 4, 67–75.
- Rabideau, S.W., 1957. The Hydrolysis of plutonium(IV). *J. Am. Chem. Soc.* 79, 3675–3677.
- Rabideau, S.W., Lemons, J.F., 1951. The potential of the Pu(III)-Pu(IV) couple and the equilibrium constants for some complex ions of Pu(IV). *J. Am. Chem. Soc.* 73, 2895–2899.

- Rai, D., 1984. Solubility Product of Pu(IV) Hydrous oxide and equilibrium constants of Pu(IV)/Pu(V), Pu(IV)/Pu(VI), and Pu(V)/Pu(VI) couples. *Radiochim. Acta* 35, 97–106.
- Rao, P.R.V., Bagawde, S.V., Ramakrishna, V.V., Patil, S.K., 1978. Sulphate complexing of some trivalent actinides. *J. Inorg. Nucl. Chem.* 40, 123–127.
- Righetto, L., Bidoglio, G., Azimonti, G., Bellobono, I.R., 1991. Competitive actinide interactions in colloidal humic acid-mineral oxide systems. *Environ. Sci. Technol.* 25, 1913–1919.
- Robouch, P., Vitorge, P., 1987. Solubility of $\text{PuO}_2(\text{CO}_3)$. *Inorg. Chim. Acta* 140 (1–2), 239–242.
- Runde, W., Reilly, S.D., Neu, M.P., 1999. Spectroscopic investigation of the formation of PuO_2Cl^+ and PuO_2Cl_2 in NaCl solutions and application for natural brine solutions. *Geochim. Cosmochim. Acta* 63, 3443–3449.
- Sakamoto, Y., Ohnuki, T., Senoo, M., 1994. Redistribution of Np(V) during the alteration of ferrihydrate. *Radiochim. Acta* 66/67, 285–289.
- Sanchez, A.L., Murray, J.W., Sibley, T.H., 1985. The adsorption of plutonium IV and V on goethite. *Geochim. Cosmochim. Acta* 49, 2297–2307.
- Sawant, R.M., Chaudhuri, N.K., Rizvi, G.H., Patil, S.K., 1985. Studies on fluoride complexing of hexavalent actinides using a fluoride ion selective electrode. *J. Radioanal. Nucl. Chem.* 91, 41–58.
- Silva, R.J., Bidoglio, G., Rand, M.H., Robouch, P.B., Wanner, H., Puigdomenech, I., 1995. *Chemical Thermodynamics of Americium*. Elsevier Science Publishing Company, Inc., New York.
- Stakebake, J.L., Larson, D.T., Haschke, J.M., 1993. Characterization of the plutonium-water reaction II: formation of a binary oxide containing Pu(VI). *J. Alloys Compounds* 202, 251–263.
- Tochiyama, O., Endo, S., Inoue, Y., 1995. Sorption of Np(V) on various iron oxides and hydrous iron oxides. *Radiochim. Acta* 68, 105–111.
- Turner, D.R., Pabalan, R.T., Bertetti, F.P., 1998. Neptunium(V) Sorption on montmorillonite: an experimental and surface complexation modeling study. *Clays Clay Min.* 46 (3), 256–269.
- Ullman, W.J., Schreiner, F., 1986. Calorimetric determination of the enthalpies of U(VI)-, Np(VI)-, and Pu(VI)- SO_4^{2-} complexes in aqueous solution at 25 °C. *Radiochim. Acta* 40, 179–183.
- Ullman, W.J., Schreiner, F., 1988. Calorimetric determination of the enthalpies of the carbonate complexes of U(VI), Np(VI), and Pu(VI) in aqueous solution at 25 °C. *Radiochim. Acta* 43 (1), 37–44.
- Zaitseva, V.P., Alekseeva, D.P., Gel'man, A.D., 1968. Hydrolysis of nitric acid solutions of plutonium(V). *Soviet Radiochem.* 10, 526–529.